Numerical modelling of the fluid-structure interaction between a stream flow and a circular cylinder

Roger Matsumoto Moreira, roger@vm.uff.br
Raphael David Aquilino Bacchi, raphadavid@gmail.com
Marcos Abreu da Silva Jr., mjuniorm@gmail.com
Erik Paim Teixeira, erikpaimteixeira@gmail.com
School of Engineering, Fluminense Federal University
R. Passos da Pátria, 156, bl.D, sl.563A, Niterói, R.J., Brazil.

Abstract. *A two-dimensional uniform incompressible flow interacting with a circular cylinder is investigated numerically, with continuity and Navier-Stokes equations being solved via a finite volume method. For validation of our numerical results, firstly a still cylinder is considered, with drag coefficients and Strouhal numbers being estimated for different Reynolds numbers. A good agreement between numerical and experimental results is found. Then the cylinder is mounted on elastic supports and is free to undergo transverse as well as streamwise excitations. The structural damping coefficient is set to zero and both transverse and in-line springs are assumed to be identical and with linear behaviour. Results are presented in terms of the cylinder displacement and vorticity fields for varying Reynolds numbers. At last, some geometry optimizations are proposed aiming to reduce the frequency of vortex shedding. Interesting features are found for the vorticity distribution at the cylinder's wake.*

Keywords: *fluid-structure interaction; vortex dynamics; finite volume method.*

1. INTRODUCTION

The study of a stream current around a circular cylinder is a classical fluid mechanics problem which has attracted the interest of several researchers since the end of the 19th century. Strouhal (1878) was the first to study the formation of vortices produced by translating cylindrical rods through air (which is the equivalent of wind blowing over a wire or a string in an Aeolian harp), followed by Rayleigh (1915) who related the Strouhal number $St\,(= fD/U)$ with the Reynolds number $Re\,(= \rho U D/\mu)$; f is the vortex shedding frequency; D, the cylinder's diameter; U, the flow velocity; ρ and μ are the fluid's density and viscosity. Re gives a measure of the ratio of inertial to viscous forces, while St is used to describe oscillating flow mechanisms. Almost after 100 years the agreement between experimental and Strouhal results in the laminar shedding regime is remarkable, with only 20% of discrepancies (see Fig. 1).

The continuous advances in computing and numerical analysis have opened new perspectives for the study of such flows, paved by theoretical and experimental studies, which include the effects of the fluid-structure interaction. The cylinder may experience unsteady hydrodynamical forces due to alternate vortex shedding and can undergo vortex induced vibrations. Also the cylinder motion can significantly alter the vortex pattern in its wake. Despite its simple geometry, it is of great interest to understand how does the structure affect its surrounding flow and vice versa. The varied physical aspects of the vortex dynamics at the cylinder's wake and its energy transfer that gives rise to modes of vibration can be found in the review papers of Williamson (1996), Williamson and Govardhan (2004) and Sarpkaya (2004). Despite the several theoretical and experimental works, the understanding of such flows is far from complete.

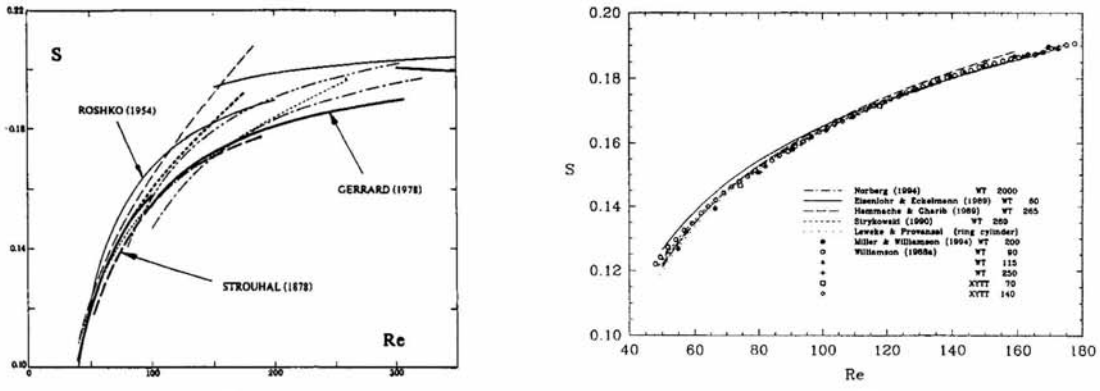

(a) (b)

Figure 1. Strouhal-Reynolds numbers relationship for a stream flow interacting with a still circular cylinder in the laminar regime: (a) Strouhal's results; (b) some recent experimental measures. (Williamson 1996)

The extensive studies of vortex-induced vibration for transverse body motions, built up over the last 35 years, remain of strong relevance compared to the case of two degrees of freedom. Nevertheless, under certain conditions, in-line vibrations may also influence the dynamics of the fluid flow and the structure. Jauvtis and Williamson (2004) observed that below a certain critical mass a rather dramatic departure occurs from previous results, which would suggest a possible modification to offshore design codes. Despite this, very few papers considering a two-degrees of freedom system for the cylinder's movement can be found in the literature. This work aims to shed further light on the subject by modelling numerically the interaction of a stream uniform flow with a circular cylinder, which is allowed to undergo transverse as well as streamwise excitations. Some geometry optimizations are then proposed aiming to reduce vortex shedding, with trajectory changes being also analysed.

2. COMPUTATIONAL MODELLING

2.1 Fluid-structure governing equations and boundary conditions

An unsteady incompressible viscous flow over a circular cylinder is modeled in two-dimensions ($x-y$ plane) with mass and momentum being conserved in the fluid domain,

$$\nabla \cdot \mathbf{u} = 0, \qquad \rho \frac{D\mathbf{u}}{Dt} = -\nabla P + \mu \nabla^2 \mathbf{u}. \tag{1}$$

$\mathbf{u}(\mathbf{x}(t))$ is the fluid's velocity; $P(\mathbf{x}(t))$ is the modified pressure; ρ and μ are the fluid's density and viscosity. Turbulence are taken into account by means of the two-equation shear stress transport model, which combines the $\kappa-\omega$ and $\kappa-\epsilon$ models, respectively, inside and outside the boundary layer. For full details see Menter (1994).

To complete our model we assume that the fluid is water ($\rho = 1,000\text{kg/m}^3$, $\mu = 0.001\text{Pa.s}$) and that initially all the fluid domain is at rest. An uniform stream flow $\mathbf{U} = (U, 0)$ is then imposed at time $t = 0$, which interacts with a cylinder of diameter $D = 0.1\text{m}$. Impermeable and no-slip boundary conditions are applied at the cylinder's surface, while far from the cylinder $\mathbf{u} \to (U, 0)$. Figure 2a illustrates the two-dimensional fluid domain with its unsteady wake downstream.

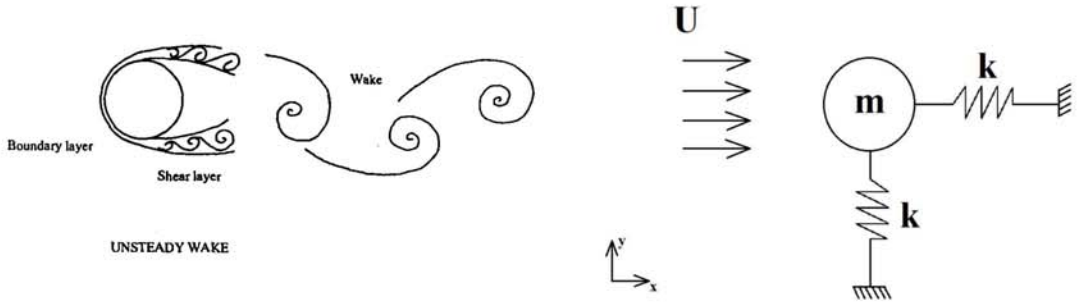

(a) (b)

Figure 2. Sketches of the 2D fluid domain with its unsteady wake (a) and the cylinder's $x-y$ motion model (b).

The fluid flow interacts with the cylinder's structure which is allowed to move in the $x-y$ plane. The cylinder is mounted on elastic supports and is free to undergo transverse as well as streamwise excitations. The structural damping coefficient is set to zero and both transverse and in-line springs are assumed to be identical and with linear behaviour. The structure's movement is modeled as a two-degrees of freedom system, as shows Fig. 2b, satisfying the following equation,

$$m\ddot{\mathbf{x}} + k\mathbf{x} = \mathbf{f}. \tag{2}$$

m and k are the cylinder's mass and stiffness; $\mathbf{x} = (x(t), y(t))$ represents the cylinder's displacement, with the upper dots representing time differentiation; $\mathbf{f} = (f_{drag}(\mathbf{x}(t)), f_{lift}(\mathbf{x}(t)))$ is the force due to the water flow, involving the time-dependent drag and lift component forces, which are computed iteratively by the flow solver. The hydrodynamic forcing will act as the coupling between the fluid and the structure equations.

2.2 CFD-structure model

The proposed boundary value problem is solved by the commercial CFD package ANSYS CFX release 12.0 (ANSYS 2009), which makes use of the finite volume method (Versteeg and Malalasekera 1995, Maliska 2004). This numerical method evaluates the conservation equations defined in §2.1 in the form of algebraic equations by calculating the velocity

and pressure fields at discrete volumes on a meshed geometry. The transport equations (1) can be represented as a set of discrete equations of a single scalar ϕ, satisfying the algebraic equation,

$$V\left(\frac{\rho^t\phi^t-\rho^{t-\Delta t}\rho^{t-\Delta t}}{\Delta t}\right)+\sum_{ip}\dot{m}_{ip}\phi_{ip}=\sum_{ip}\left(\Gamma_{eff}\frac{\partial\phi^t}{\partial x_j}\Delta n_j\right)_{ip}+S_\phi V, \tag{3}$$

where V represents the control volume; Δt is the time step; the index ip references the quantity to the integration points in each control volume face; $\dot{m}=\rho U_j\Delta n$; Δn represents the outward normal to the control volume surface; Γ_{eff} is the diffusion coefficient; $S_\phi V$ is the source term.

The general transport equation (3) is solved for different entities represented by ϕ. A second-order backward Euler discretization is applied to the transient term; a pseudo-second order scheme for advective terms in momentum and turbulence equations is also employed. Figure 3 shows one of the computational grids used, which contains 23,605 hexahedral elements. Tetrahedral elements were also employed such as in the presence of plates attached to the cylinder. Despite the semi-circular inlet at the left side of the fluid's domain, in this paper only uniform stream flows are considered i.e. $\mathbf{U}=(U,0)$. All the computations were carried out on a 64 bit, 2.40 GHz Intel Quad Core processor with 8 Gb of RAM.

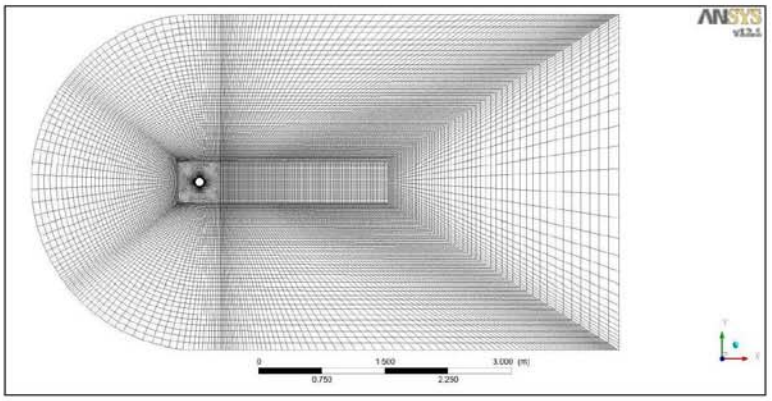

Figure 3. Computational grid.

Equation (2) is also represented with a discrete formulation in time, which in Einstein's notation gives,

$$x_i^t=\frac{f_i^t+m\left(\frac{x_i^{t-1}}{\Delta t^2}+\frac{\dot{x}_i^{t-1}}{\Delta t}\right)}{\frac{m}{\Delta t^2}+k}, \tag{4}$$

with the superscripts representing time. The hydrodynamical forces f_i^t are determined by ANSYS CFX solver at the end of each time step, enabling the calculation of the cylinder's position for the next time step. Due to the cylinder's motion, the CFD-solver displaces its mesh and applies a zero-divergence equation for the product of the displacement vector and the mesh stiffness to obtain the displacement in each mesh node. The mesh stiffness increases in value according to the size of each element in order to avoid errors in the topology. More details can be found in ANSYS (2009) and Teixeira and Silva Jr. (2010).

3. NUMERICAL RESULTS

Results are compiled in the following subsections. For validation of numerical solutions, a circular cylinder with no displacement is considered at first, with only fluid-flow variables being determined for varying Reynolds numbers. Then the fluid-structure model proposed in §2 is solved for four cases of interest (see Tab. 1). Finally some geometry optimizations are proposed in the last subsection aiming to reduce the frequency of vortex shedding with some conclusions being addressed.

3.1 Still circular cylinder

Before we start a more complex analysis, computations were done at various Reynolds numbers considering the classical problem of a stream flow over a circular cylinder at rest. Numerical and experimental results (extracted from

Table 1. Fluid and structure properties for a moving circular cylinder.

Properties	Case 1	Case 2	Case 3	Case 4
U (m/s)	0.022	0.044	0.044	1.100
Re	2,200	4,400	4,400	110,000
k (N/m)	30.0	30.0	300.0	236.0
m (kg)	0.2	0.2	0.2	66.3
St	0.2087	0.2174	0.2174	0.2273

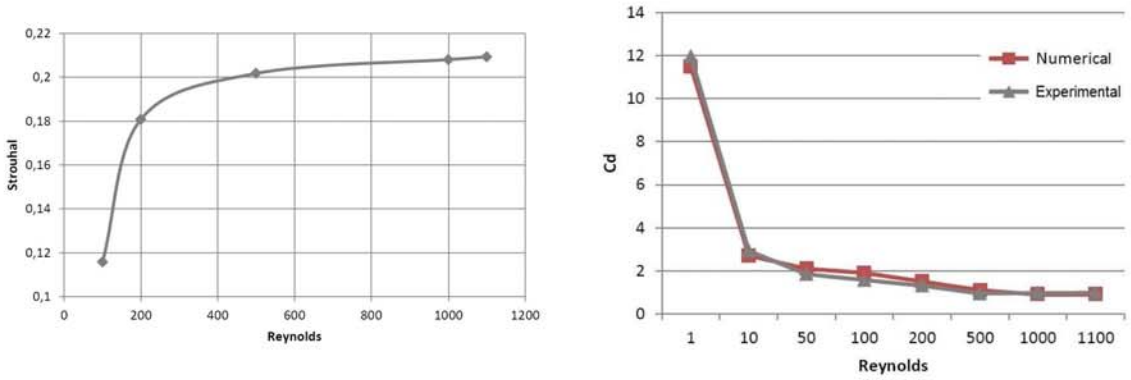

(a) (b)

Figure 4. Comparison between experimental and numerical results for a stream flow interacting with a still circular cylinder: (a) St versus Re; (b) C_d versus Re.

Schlichting 1968) are compared in Fig. 4 in terms of the relationship of the Strouhal number (St) and the drag coefficient (C_d) with the Reynolds number (Re). A good agreement was found in both graphs. As Re increase in the laminar regime, C_d rapidly decrease until the turbulent regime is reached, with C_d decaying very slowly from there. The numerical behaviour of the Strouhal number also follows the experimental results, with a practically constant $St \approx 0.21$ for $500 \leq Re \leq 5,000$.

3.2 Moving circular cylinder

If otherwise a coupled fluid-structure model is applied as explained in §2, the hydrodynamical forcing will disturb the quiescent cylinder, causing its displacement, which will affect the surrounding fluid-flow. Figure 5 shows the cylinder's trajectories and vorticity distributions for Cases 1 and 2 (listed in Tab. 1) after a total time of 510.8s. If a cylinder is free to oscillate in both the transverse and in-line directions, the common frequencies of the body and the driving forces in their respective directions may lead to lock-in and the axis of the body traces the path of figure-eight, as shows the left column of Fig. 5. Indeed, Moe and Wu (1990), Moe *et al.* (1994) and Sarpkaya (1995) found that the common figure-eight loop is caused by the considerable variation of drag force during large amplitude oscillation, though other displacement shapes were also observed for different Reynolds numbers (Chen and Jendrzejczyk 1979, Jauvtis and Williamson 2004). Displacements were also magnified as the Reynolds number increases. Regarding the vortex dynamics, an insignificant rise in the vortex shedding frequency was associated with the increase of Re. As we increase the stiffness (see Case 3 in Tab. 1 and Fig. 6), the cylinder's displacement decreases, with the figure-eight shape being slightly distorted when compared to lower stiffnesses.

3.3 Geometry optimizations

The installation of plate devices surrounding the riser's structure aiming to minimize fluid-flow vibrations is an option in the offshore petroleum industry. In this sense the geometry is modified in our problem by introducing a single plate downstream the cylinder (Fig. 7, Case 5) and a set of three plates symmetrically distributed onto the cylinder's surface (Fig. 7, Case 6). For comparison purposes, Fig. 7 also shows the corresponding trajectory and vorticity distribution for a cylinder without any plate (Case 4 in Tab. 1).

The numerical results show that these devices can reduce significantly the frequency of vortex shedding, from 2.500Hz in Case 4 to 0.272Hz in Case 5 and to astonishing 0.055Hz in Case 6. The vorticity fields plotted in the right-column of Fig. 7 shows how these structures affect the vortex dynamics at the cylinder's wake, though displacements are also

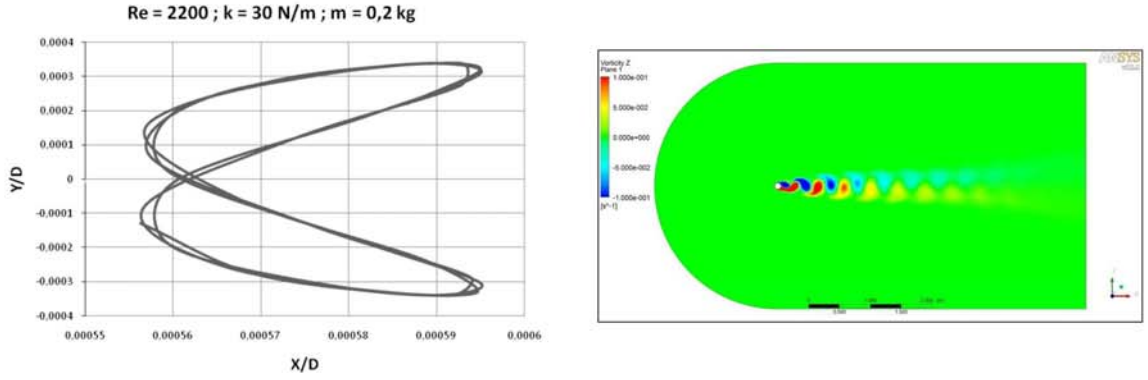

Case 1

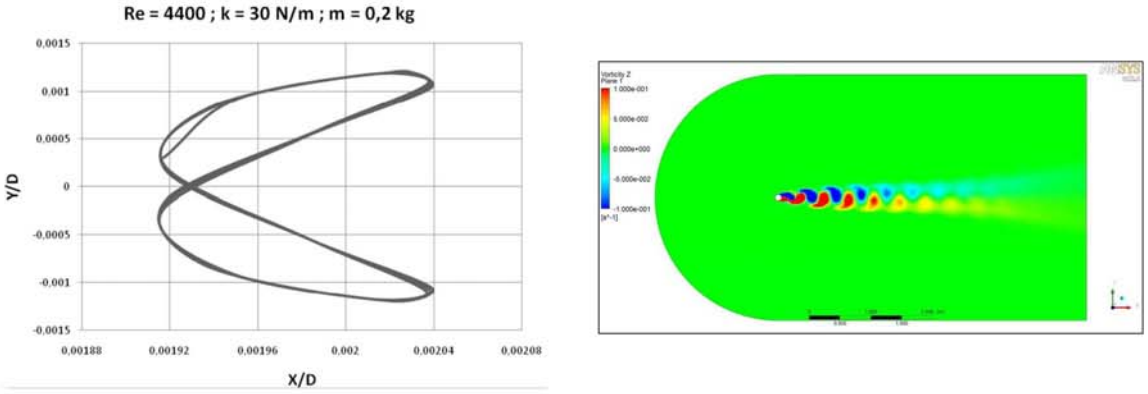

Case 2

Figure 5. Trajectory (left column) and vorticity distribution (right column) due to a stream flow interacting with a moving circular cylinder ($k = 30$N/m, $m = 0.2$kg). Case 1: $Re = 2.2\times10^3$; $St = 0.2087$. Case 2: $Re = 4.4\times10^3$; $St = 0.2174$.

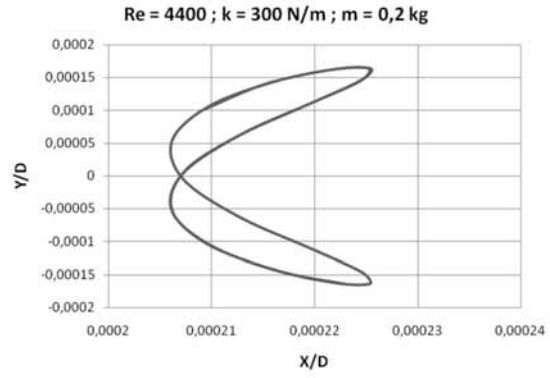

Case 3

Figure 6. Trajectory due to a stream flow over a moving circular cylinder ($k = 300$N/m, $m = 0.2$kg). Case 3: $Re = 4.4 \times 10^3$, $St = 0.2174$.

augmented depending on the plates arrangement (see the left-column of Fig. 7). As expected drag forces depends now on the angle of incidence between the stream flow and the plates configuration. Note also that the cylinder's paths are significantly changed by its geometry, with the common figure-eight loop no more being observed, even for Case 4. Indeed Chen and Jendrzejczyk (1979) and Jauvtis and Williamson (2004) showed that other displacement shapes can be observed for different Reynolds numbers.

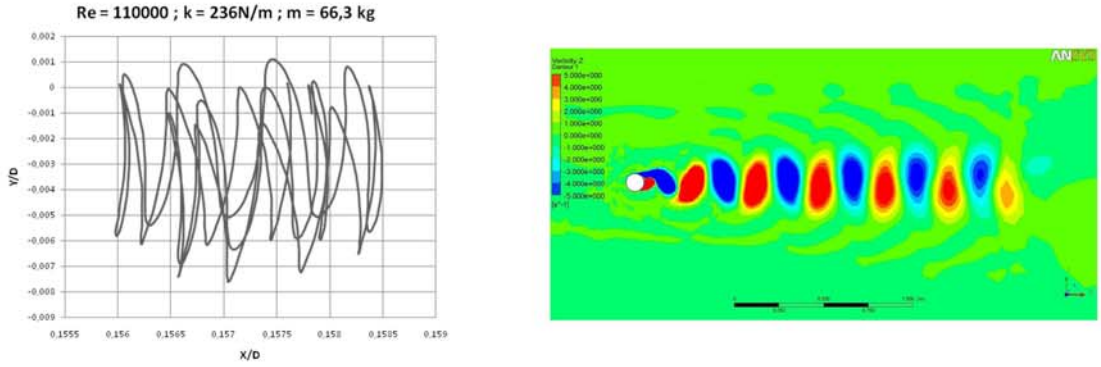

Case 4

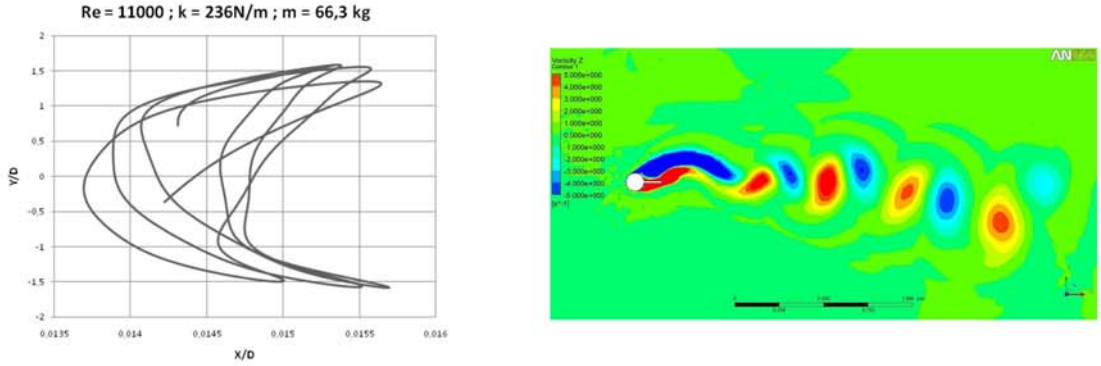

Case 5

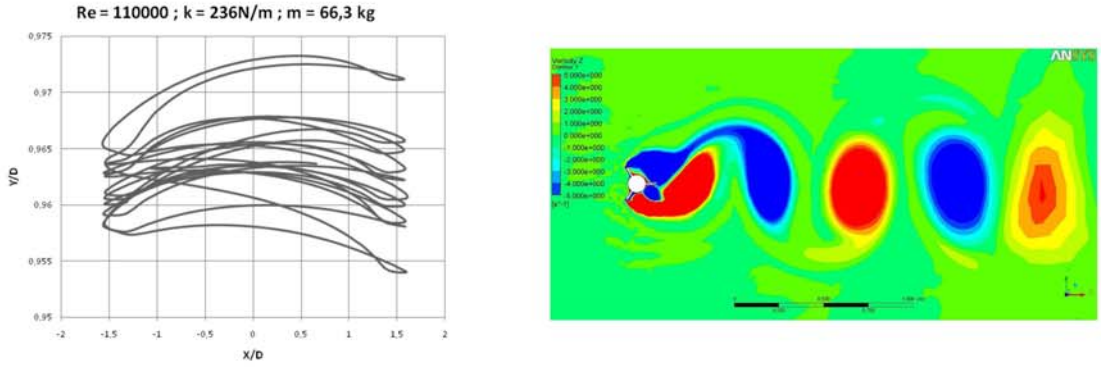

Case 6

Figure 7. Trajectory (left column) and vorticity distribution (right column) due to a stream flow ($Re = 1.1 \times 10^5$) interacting with a moving circular cylinder ($k = 236$N/m, $m = 66.3$kg). Case 4: without any plate; $St = 0.2273$. Case 5: with a single plate downstream; $St = 0.0247$. Case 6: with 3 plates symmetrically distributed; $St = 0.0050$.

4. CONCLUSIONS

A good agreement between numerical and experimental results (extracted from Schlichting 1968) is found for a quiescent circular cylinder in a stream flow. For a moving circular cylinder with two degrees of freedom and no geometry optimization, figure-eight paths are found for Re equal to 2.2×10^3 and 4.4×10^3, with $St \approx 0.21$, which agree qualitatively with the works of Moe and Wu (1990), Moe *et al.* (1994) and Sarpkaya (1995). As the Reynolds number increases ($Re = 1.1 \times 10^5$), other displacement shapes are observed followed by a small increase in the Strouhal number ($St = 0.2273$), such as found by Chen and Jendrzejczyk (1979) and Jauvtis and Williamson (2004). The introduction of plate devices surrounding the cylinder's structure proves to be effective for reducing the frequency of vortex shedding, though displacements are also augmented due to its associated increase in its drag force.

5. ACKNOWLEDGEMENTS

R.M.Moreira acknowledges the financial support through CNPq, the national research and development council (contract number 62.0018/2003-8-PADCT III / FAPERJ).

6. REFERENCES

ANSYS CFX 12.0, 2009, "ANSYS CFX user's guide", ANSYS Inc.

Chen, S.S. and Jendrzejczyk, J.A., 1979, "Dynamic response of a circular cylinder subjected to liquid cross flow", J. Pressure Vessel Tech., v.101, pp.106-112.

Jauvtis, N. and Williamson, C.H.K., 2004, "The effect of two degrees of freedom on vortex-induced vibration at low mass and damping", J. Fluid Mech., v.509, pp.23-62.

Maliska, C.R., 2004, "Transferência de calor e mecânica dos fluidos computacional", 2nd ed., LTC, Brazil, 472p.

Menter, F.R., 1994, "Two-equation eddy-viscosity turbulence models for engineering applications," AIAA Journal, v.32, no.8, pp.1598-1605.

Moe, G. and Wu, Z.-J., 1990, "The lift force on a cylinder vibrating in a current", ASME J. Offshore Mech. Arctic Engng., v.112, pp.297-303.

Moe, G., Holden, K. and Yttervoll, P.O., 1994, "Motion of spring supported cylinders in subcritical and critical water flows", Proc. 4th Internat. Offshore Polar Engng. Conf., Osaka, pp.468-475.

Rayleigh, Lord, 1915, "Aeolian tones", Phil. Mag., pp.29-433.

Sarpkaya, T., 1995, "Hydrodynamic damping, flow-induced oscillations, and biharmonic response", ASME J. Offshore Mech. Arctic Engng., v.117, pp.232Ű238.

Sarpkaya, T., 2004, "A critical review of the intrinsic nature of vortex-induced vibrations", J. Fluids Struct., v.19, pp.389-447.

Schlichting, H., 1968, "Boundary-Layer Theory", 6th ed., McGraw-Hill Book Co.

Strouhal, V., 1878, "Uber eine besondere Art der Tonerregung", Ann. Phys. Chem. (Liepzig), v.10, pp.5-216.

Teixeira, E.P. and Silva Jr., M.A., 2010, "Numerical modelling of the fluid-structure interaction of a riser", Undergrad. Monograph, Mech. Engng. Dep., Fluminense Federal University, Brazil.

Versteeg, H.K. and Malalasekera, W., 1995, "An introduction to computational fluid dynamics: the finite volume method", Pearson Prentice-Hall, 257p.

Williamson, C.H.K., 1996, "Vortex dynamics in the cylinder wake", Annu. Rev. Fluid Mech., v.28, pp.477-539.

Williamson, C.H.K. and Govardhan, R., 2004, "Vortex-induced vibrations", Annu. Rev. Fluid Mech., v.36, pp.413-455.

7. Responsibility notice

The authors are the only responsible for the printed material included in this paper.